





Article

Human Activities Introduced Degenerations of Wetlands (1975–2013) across the Sanjiang Plain North of the Wandashan Mountain, China

Jing Xie ^{1,†} , Yeran Sun ^{2,†} , Xiao Liu ^{3,4,5,6,*} , Zhi Ding ⁷ and Ming Lu ⁸ 

- ¹ School of Geographical and Earth Sciences, University of Glasgow, Glasgow G12 8QQ, UK; jing.xie@glasgow.ac.uk or jing.xie@geo.uzh.ch
- ² Department of Geography, College of Science, Swansea University, Swansea SA2 8PP, UK; yeran.sun@swansea.ac.uk
- ³ School of Architecture, South China University of Technology, Guangzhou 510641, China
- ⁴ Department of Urban Planning and Design, Faculty of Architecture, The University of Hong Kong, Hong Kong 999077, China
- ⁵ Architectural Design & Research Institute Co., Ltd., South China University of Technology, Guangzhou 510641, China
- ⁶ State Key Laboratory of Subtropical Building Science, South China University of Technology, Guangzhou 510641, China
- ⁷ Chongqing Jinpo Mountain Karst Ecosystem National Observation and Research Station, School of Geographical Sciences, Southwest University, Chongqing 400715, China; dingzhi11@mails.ucas.ac.cn
- ⁸ Qian Xuesen Laboratory of Space Technology, Beijing 100094, China; luming@qxslab.cn
- * Correspondence: xiaoliu@hku.hk or xiaoliu@scut.edu.cn
- † These authors contributed equally to this study and shared the first authorship.



Citation: Xie, J.; Sun, Y.; Liu, X.; Ding, Z.; Lu, M. Human Activities Introduced Degenerations of Wetlands (1975–2013) across the Sanjiang Plain North of the Wandashan Mountain, China. *Land* **2021**, *10*, 1361. <https://doi.org/10.3390/land10121361>

Academic Editors: Baojie He, Ayyoob Sharifi, Chi Feng and Jun Yang

Received: 24 November 2021
Accepted: 7 December 2021
Published: 9 December 2021

Publisher's Note: MDPI stays neutral with regard to jurisdictional claims in published maps and institutional affiliations.



Copyright: © 2021 by the authors. Licensee MDPI, Basel, Switzerland. This article is an open access article distributed under the terms and conditions of the Creative Commons Attribution (CC BY) license (<https://creativecommons.org/licenses/by/4.0/>).

Abstract: Human-induced dramatic loss and fragmentation of wetlands need further understanding through historical backtracking analysis at a geographical landscape scale. In this study, we investigated time-series wetlands maps from 1975, 1983, 1989, 2000, 2006, and 2013 derived from Landsat images based on the object-oriented classification of wetlands across the Sanjiang Plain north of the Wandashan Mountains. The spatial and temporal changes in the wetlands that occurred at different time periods and the Euclidean distances between artificial land-use types and natural land-cover areas were evaluated for their impact. Our results showed that wetland was the dominant landscape in 1975; however, arable land became the main land coverage in 2013 owing to severe changes in agricultural development over the past decades. The closer to arable land, the greater the wetland loss during the entire investigated period; agriculture activities were the dominant driving force for the degradation of wetlands based on landscape changes; secondary was the rapid expansion in building land use (i.e., human settlement, transportation, and establishment of irrigation canals). More specifically, the rapid loss of wetland areas over 1975–2000 was mainly owing to extensive agricultural reclamation. The mitigated loss of wetland areas over 2000–2013 was because of the protection and restored implementation of wetlands under governmental policies. The wetlands of the study area suffered severe human disturbance, and our analysis may help explain the loss process of wetlands, but more effective management and administration is still needed to address the issues around the balance between agricultural production and wetland protection for further sustainable development.

Keywords: wetlands; human activities; land use land cover; object-oriented classification; Sanjiang Plain

1. Introduction

Wetlands are constitutive components of global ecosystems, providing essential habitats for both flora and fauna and supporting a high diversity of plants and wildlife

species [1,2]. Though occupying less than 6% of land surface area, many critical functions and services are provided by wetlands [3], such as water supplies, carbon storage, and habitats for wildlife, etc. [4,5]. A number of studies have shown that changes in wetlands contribute to climate change from a regional to a global scale [6,7] and directly impact worldwide biotic diversities [8,9]. To better protect our living environment in cities and the countryside [10,11] by following the United Nations sustainable development goals, it is important to perform detailed quantitative investigation of meaningful spatiotemporal views [12–14].

Wetland ecosystems are reported to be very susceptible to climate change, and the changing climate is projected to markedly affect wetland ecosystems [8]. Both temperature increases and precipitation decreases can result in wetland loss and degeneration [2,15]. Warming climate change can result in precipitation decrease and/or increase, causing the degradation of wetlands owing to the depleted environment, particularly from the reduction in water support [16]. However, these studies focused on either natural effects or human activities in the time series; quantitative research on the effect of human activities on wetland degradation in view of land-use/land-cover (LULC) change in the Sanjiang Plain using remote sensing is scarce.

Sanjiang Plain is one of the most worthwhile examples of monitoring the change in wetlands by remote sensing (see Figure 1); it includes two internationally important reserves with Ramsar site numbers: Sanjiang National Nature Reserve (SNNR) and Honghe National Nature Reserve (HNNE) [17]. Sanjiang Plain was once the largest freshwater wetland [3] but is now second to the Qinghai–Tibet Highland wetland [18]. From the 1950s to the 2000s, the Sanjiang Plain has experienced the severe, dramatic changes of LULC [9,15]. Large-scale agricultural development has been mainly responsible for the 77% loss of wetlands [5], and the wetland landscapes in this area have been severely fragmented by intensive human activities [5,19,20]. The wetland changes across the Sanjiang Plain are a hot research topic [18,20], and a number of studies have paid attention to the wetland changes in the area [2,5,12,13,18,19].

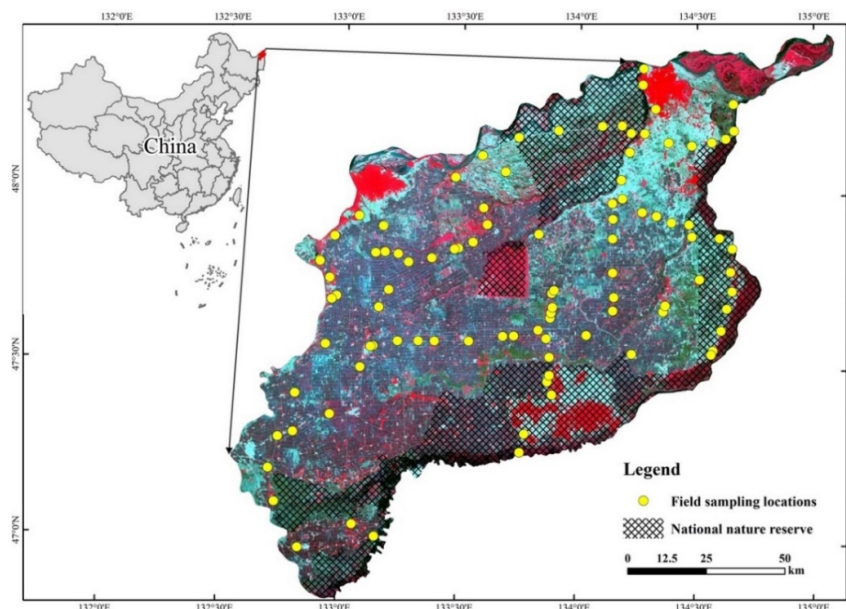


Figure 1. Location of the study area (illustrated by Landsat images with RGB (4, 3 and 2 bands)), the Sanjiang Plain north of the Wandashan Mountain in northeast China; field survey locations are unified for comparison between different investigated years (1975–2013).

In Sanjiang Plain, LULC dynamics were reported to be mainly derived from economics and policies [2,5]. Eight more new farms were built and 7317 km² of wetlands were lost from 1965 to 1976 in the small Sanjiang Plain [15]. Based on this, we chose the Sanjiang Plain

north of the Wandashan Mountains [12,21] for our research site. Contrasting landscape structure and analyzing the characteristics of wetland change under the impact of human activities on this area are still narrowly focused on the field. The ecological communities are affected by the direct, indirect, and cumulative impacts of land use [22–24]. Wetland ecology is also strongly related to the human activity occurring in the surrounding landscapes [5,12]. For example, roads can significantly reduce wetland habitat biodiversity [25] at distances of more than 1 km from the roadway [26]. While the Sanjiang plain had experienced consistent losses before 2010 [2], degradation of wetlands dominated by human activities tended to slow down in the 2010s owing to the protection and restored implementation [14,22,27]. We thus selected the different time periods between 1975 and 2013 to investigate time-series changes of LULC and their association with wetland degradation.

The remote sensing (RS) and geographic information system (GIS) methods used for historical imagery are powerful tools for LULC change analysis. To date, a number of studies have applied remote sensing, GIS, and statistical methods to study the relation between LULC change and human activities. The repeated RS monitoring greatly facilitates studies of landscape change over large areas and locations in remote areas or with difficult ground access [28–33]. For instance, RS Landsat series images combining object-based classification were studied for differing wetland changes and proximate causes in the Amur River Basin between Russia and China [14]. Meanwhile, based on RS Landsat data and GIS spatial analysis, both anthropogenic and natural drivers of long-term wetland changes were also analyzed across the Amur River Basin on the Chinese side [27]. For mapping national wetlands in China, RS and GIS data provided essential information for the analysis of coastal ecosystems [13,34]. Thus, RS and GIS techniques are good ways to obtain available geographic information to assess the effect of human activities on the surrounding landscapes.

In this paper, to better understand the spatiotemporal dynamics and degradation of wetlands, the temporal changes to wetlands across the Sanjiang Plain north of the Wandashan Mountains were examined with the following objectives: (1) to investigate LULC changes over six temporal points ranging from 1975 to 2013 using Landsat remote sensing data, GIS, and quantitative analysis; (2) to analyze the temporal changes in wetland and landscape; and (3) to quantitatively assess the impact of human activities on the degradation of these inland wetlands.

2. Material and Methods

2.1. Study Area

The selected study area in the Sanjiang Plain north of the Wandashan Mountains ($46^{\circ}48'5.83'' \sim 48^{\circ}29'16.43''$ N, $132^{\circ}26'25.52'' \sim 135^{\circ}7'24.4''$ E) covers the northeastern portion of Heilongjiang province, China, that lies within the low-lying areas of the Sanjiang Plain and occupies an area of approximately 16,070 km² (Figure 1) and four counties. Surrounding the Nong River, it includes the Honghe National Nature Reserve located in the headwaters and the Sanjiang National Nature Reserve located in the lower reaches [20]. With an elevation of <150 m above sea level in most areas, the study regions are mainly the low alluvial plains surrounded by the Heilong, Songhua, and Wusuli Rivers [35]. With a frost-free season ranging between 120 and 140 days, the climate of this region varies from temperate-humid to sub-humid continental monsoon. In general, the annual mean temperature is 3.2 °C, and the mean temperature is 20.5 °C in the coldest January and 21.7 °C in the hottest July. Annual precipitation ranges between 500 and 650 mm and occurs mainly between May and September. In the area, *Carex* marsh is the main wetland plant, while there are little shrub wetlands in the national nature reserve and forest wetlands adjacent to the rivers' banks in the study area [21]. Since the 1950s, large areas of wetlands have been converted to arable lands because of the grain production policy [5]. In the period from 1968 to 1972, thousands of urban educated youths responded to the "Going to the Countryside and Settling in the Communes" exhortation of government during the

Great Cultural Revolution and were assigned to the Sanjiang Plain to develop agriculture. Currently, dominated agriculture land is the paddy field.

2.2. Dataset and Preparation

In the study area, a set of 18 cloud-free satellite scenes (Table A1 shows detailed description) were collected from the USGS Earth Resources Observation and Science Center (<http://glovis.usgs.gov>, accessed 15 March 2014) from May to September, covering the season of growing days for each studied year. These comprised Landsat Multispectral Scanner (MSS) data (80 m scale), Landsat Thematic Mapper (TM) data (30 m scale), Enhanced Thematic Mapper (ETM+), and Landsat 8 data (30 m scale). Each image was projected into the World Geodetic System 1984 coordinate system and Universal Transverse Mercator Zone 53 North. The ENVI/IDL (version 5.3, the EXELIS Inc., McLean, VA, USA) was employed to resample MSS images to 30 m resolution at a pixel level with the nearest neighbor method. Finally, the images were imported and stored in *.tif format for the object-oriented classification.

A total of 428 field sampling locations and their landscape information were collected for the 2013 LULC classification assessment from field surveys in 2012 and 2013. Global positioning satellite (GPS) measurements utilized a random stratified sampling scheme to ensure >10 samples for each class. For the 1975, 1983, 1989, 2000 and 2006 classification assessments, historical field samples and field survey routing lines, and auxiliary data (including the vegetation maps at a scale of 1:250,000 and counties' land-use/land-cover maps with a scale of 1:100,000) were collected (corresponding to the same locations/coordinates of 2013) for accuracy assessment.

2.3. Land-Use/Land-Cover (LULC) Mapping

The classification scheme consisted of 10 types: (1) wetland, (2) river, (3) lake, (4) canal, (5) woodland, (6) meadow, (7) arable land, (8) residential land, (9) transportation land, and (10) barren land, which were classified and identified for the LULC result. The object-oriented classification method was employed for LULC mapping. The object-oriented classification used approaches as described in Xie et al. (2012) [21] for detailed remote sensing image classification. Multi-resolution segmentation chosen for this classification was a bottom-up region merging method [36]; spectral, geometric, and statistical characteristics, and relationships between linked levels of the image objects could then be employed for classification [37].

The mapping processing was clustered into three categories: (i) segmentation to create imagery objects at multiple scales (50-pixel scale for the classification rule test, and 10- and 5-pixel scales for the final classification application), (ii) LULC classification based on object-oriented patterns using spectral, index, textural, and spatial features of images, and (iii) its accuracy assessment based on field investigation. According to attributes of the object features, the classification of an object was determined using a number of decision rules. Each of the images was classified separately based on its adapted thresholds using decision rules, and the classification results were merged in each investigated year in the ArcGIS environment. The Kappa coefficient was also computed to assess the accuracy of the classification result. The segmentation and object-based classification was carried out using eCognition Developer software 5.2 (Definiens Imaging, München, Germany). The classification accuracies for 10 categories of LULC of the object-oriented classification method over the 6 periods all exceeded 75.0% (see Table A2).

2.4. Spatial and Temporal Changes of Wetlands

Landscape indices involving quantitative measurements were employed for analyzing landscape changes over the study period in LULC types expressing the structures and the fragmentations of the landscape patterns as a whole for the entire study area. Considering the scale of the analyses and the objectives of the study, eight landscape indices were chosen as the appropriate landscape pattern indices, which are often employed in studies

of landscape ecology, were adapted in this study. They were largest patch index (LPI), mean of shape index (SHAPE_MN), mean of fractal dominance index (FRAC_MN), mean of contiguity index (CONTIG_MN) [38], patch density (PD), patch cohesion index (COHESION), Shannon’s diversity index (SHDI) [39], and Shannon’s evenness index (SHEI) [38]. The details of the computation and the reasonable range of each employed index are summarized in Table 1. These landscape indices can quantitatively measure the structure and fragmentation of the landscape patterns as a whole. The spatial analyses of the eight landscape indices were carried out using ArcGIS 10.0 software (ESRI, Redland, CA, USA). Fragstats 4.2 (<http://www.umass.edu/landeco/index.html>, accessed 15 March 2014) was employed to estimate the landscape indices.

Table 1. Description of selected landscape metrics for landscape pattern analysis in this study.

Landscape Indices	Algorithm	Value Range
LPI	$LPI = (\max(a_{ij}) / A)$	$0 < LPI \leq 100$
SHAPE_MN	$SHAPE = (\sum_{i=1}^n \sum_{j=1}^m (0.25p_{ij} / \sqrt{a_{ij}}) / N)$	$SHAPE \geq 1$, without limit
FRAC_MN	$FRAC_MN = 2 \ln(0.25P_{ij}) / \ln a_{ij}$	$1 \leq FRAC \leq 2$
CONTIG_MN	$CONTIG_MN = ((\sum_{r=1}^z c_{ijr} / a_{ij}) - 1) / (V - 1)$	$0 \leq CONTIG \leq 1$
PD	$PD = N / A$	$PD \geq 0$, without limit
COHESION	$COHESION = (1 - \sum_{j=1}^m p_{ij} / \sum_{j=1}^m p_{ij} \sqrt{a_{ij}}) (1 - 1 / \sqrt{N})^{-1}$	$0 \leq COHESION \leq 100$
SHDI	$SHDI = - \sum_{i=1}^R (P_i * \ln P_i)$	$SHDI \geq 0$, without limit
SHEI	$SHDI = - \sum_{i=1}^R (P_i * \ln P_i) / \ln R$	$0 \leq SHEI \leq 1$

Note: *, a_{ij} , multiplication sign in Equation; the area of the j_{th} patch belonging to the i_{th} landscape; A , sum of a landscape area; P_{ij} , the eventuality of the j_{th} patch belonging to the sum of the i_{th} landscape area; N , number of total patches in a landscape; C_{ijr} , contiguity value of the pixel r in the i_{th} patch; V , value in a template of 3×3 cells; P_i , the eventuality of the i_{th} landscape type to the summation of the landscape area; R , summation of types totally in the landscapes; z , total number of pixel in the i_{th} patch.

2.5. Human Activities Effect Assessment

Many factors can affect the landscape of wetlands. In general, wetland changes have been tightly associated with various natural environment factors (e.g., geomorphology, hydrology, and climate, etc.). In addition, human activities (e.g., per capita GDP, densities of population and agricultural population, etc.) have also greatly affected wetlands. Owing to the short study period, 1975–2013, natural environment factors remained relatively stable compared with frequent human activities. We also learned the climate (annual temperature, precipitation, evapotranspiration, and dryness) underwent no significant changes from the 1970s to 2010 in the Sanjiang Plain [5]. Human activities, such as agricultural produce, economics, policies, and so on, are the major driving forces for LULC dynamics in the Sanjiang Plain [5,12], and LULC experienced significant changes and had a critical influence on wetland changes. We also did not consider quantitative human factors such as the population, agricultural population density, and economic growth.

Linear and curvilinear regression analysis (e.g., simple linear regression, quadratic regression, and logistic regression, etc.) were employed to explore the relationships of wetland degradation with other LULC variables derived from Landsat image pixels. The proximity to every landscape was measured with nine land-cover factors that helped to identify the effect of human accessibility on the wetland loss. Hence, nine variables (e.g., interval wetland pixel reduction distances to river, lake, canal, woodland, meadow, arable land, residential land, transportation land, and barren land) were used to analyze their impact on the wetland changes of each pixel from the nearest landscape (km) across the study areas.

The Landsat data sets for six periods (1975–1983, 1983–1989, 1989–2000, 2000–2006, 2006–2013 and 1975–2013) were converted into grid data with raster data sets (30 m

spatial resolution), and then the Euclidean distances (<http://resources.arcgis.com>, accessed 15 March 2021) to the other nine variables were computed using GIS spatial analysis methods. To ensure that the spatial effects of LULC change could be analyzed, all pixels of the marsh degradation and the nine other LULC variables were used to estimate the coefficients. Each independent variable was normalized to differentiate its relative effect as a driving force in the degradation of wetlands. The maps of wetland degradation in the test region were produced in the ArcGIS 10.0 software package. Finally, the degradation pixels of wetlands and their distances to other variables were measured by linear and nonlinear regression analyses to identify the relationships between wetland loss and other LULC changes using Origin 8.1 and SPSS 19.0.

3. Results

3.1. Land-Use/Land-Cover (LULC) Dynamics (1975–2013)

Wetlands in the study area experienced continuous loss over the entire investigated period (i.e., 1975, 1983, 1989, 2000, 2006, and 2013) in the Sanjiang Plain north of the Wandashan Mountains (Figure 2). Wetland degradation was extremely harsh from 1976 to 2000, decreasing from 63.0% of the total area to 19.8% (Table 2). In 1975, wetlands covered 10,126.18 km² but then decreased to 47.7, 35.6, 19.8, and 14.2%, respectively, in 1983, 1989, 2000, and 2006. The remaining wetlands were approximately 13.8% (2214.80 km²) in 2013 with an average annual loss of 208.19 km² in wetland areas between 1975 and 2013. However, the speed of wetland loss tended to slow down over time. More specifically, the average annual reduction in wetlands was approximately 308.89 km² during 1975–1983, 323.71 km² during 1983–1989, 229.69 km² during 1989–2000, 151.90 km² during 2000–2006, and 8.57 km² during 2006–2013 (Table A4). Compared to the loss of wetland area during 1975–2000, the rate of degradation during 2000–2013 was obviously slower than in years before 2000 and this reduced loss was owing to the effort at wetland protection.

In contrast, arable land across the study area showed a continuous increase over the investigated period, from 3321.36 km² (20.7% of total area) in 1975 to 11,401.05 km² (71.0%) in 2013. Arable land had a mean annual increase rate of 1.7% during 1975–1983, 2.7% during 1983–1989, 1.5% during 1989–2000, 1.0% during 2000–2006, 0.3% during 2006–2013, and 1.3% during 1975–2013. Similar to the increased area of arable land, canals increased continuously for nearly 40 years, from 4.44 km² in 1975 to 58.80 km² in 2013, with an average annual 1.43 km² increase during 1975–2013 (Table A3).

The areas of residential and transportation lands consecutively increased over the study period (Table A4). Residential land area increased from approximately 27.88 km² (0.2%) in 1975 to 157.56 km² (1.0%) in 2013, and the transportation land increased slightly from 37.37 (0.2%) to 173.94 km² (1.1%) in the same time intervals. Meadow decreased from approximately 863.35 km² (5.4%) in 1975 to 281.43 km² (1.8%) in 2013, in total, 581.92 km² over the past 38 years. The average annual areal decrease in meadow was approximately 67.40 km² (0.2%). This average change rate differed over five time-interval stages, being 0.3, −1.2, 0.1, −0.2, and 0.2% during 1975–1983, 1983–1989, 1989–2000, 2000–2006, and 2006–2013, respectively. By 1989, the lost meadow had mainly been transformed to arable land and the proportion of meadow decreased to only 0.6% of the original area. There was virtually no meadow remaining after 1989 (Table A4).

The areas of woodland, river, lakes, and barren land did not experience a large change from 1976 to 2013, approximately 1249.39 (7.8%), 392.1 (2.4%), 31.1 (0.2%), and 12.8 km² (0.1%), respectively, in 1975, and approximately 1393.27 (8.7%), 359.1 (2.2%), 29.5 (0.2%), and 3.02 km² (0.0%), respectively, in 2013 (Table A4). Changes of LULC in the study area differed over the six-time intervals. Most LULC types varied especially over 1975–2000 but slowed down after 2000.

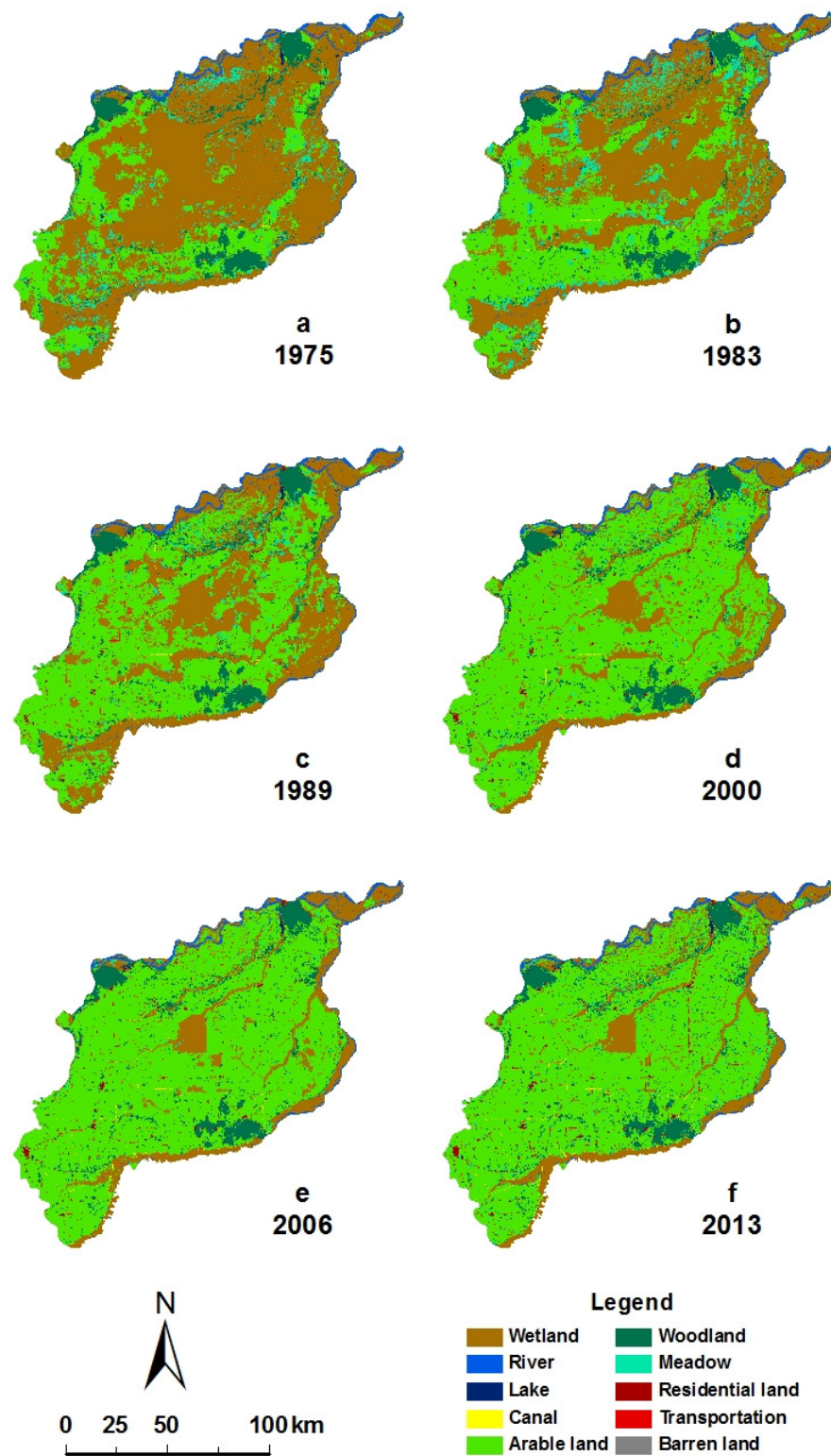


Figure 2. Changes in wetlands cover in the Sanjiang Plain north of the Wandashan Mountains, China, in 1975 (a), 1983 (b), 1989 (c), 2000 (d), 2006 (e), and 2013 (f).

Table 2. Land-use/land-cover (LULC) area extent (%) of the main LULC classes over the period 1975–2013 (area in km²).

LULC Types	1975		1983		1989		2000		2006		2013	
	Area	%	Area	%	Area	%	Area	%	Area	%	Area	%
Wetland	10,126.18	63.0	7655.04	47.6	5712.79	35.6	3186.22	19.8	2274.79	14.2	2214.80	13.8
River	392.09	2.4	358.90	2.2	392.09	2.4	334.61	2.1	348.60	2.2	359.11	2.2
Lake	31.09	0.2	19.77	0.1	20.72	0.1	33.59	0.2	32.23	0.2	29.46	0.2
Canal	4.44	0.0	16.03	0.1	23.02	0.1	34.44	0.2	45.02	0.3	58.80	0.4
Woodland	1249.39	7.8	1238.85	7.7	1292.55	8.1	1244.08	7.7	1272.84	7.9	1393.27	8.7
Meadow	863.35	5.4	1239.18	7.7	412.00	0.6	291.43	1.8	103.32	0.6	281.43	1.8
Arable land	3321.36	20.7	5442.57	33.9	8015.83	49.9	10,733.68	66.8	11,721.14	73.0	11,401.05	71.0
Residential land	27.88	0.2	42.94	0.3	88.29	0.6	117.40	0.7	137.51	0.9	157.56	1.0
Transportation land	37.37	0.2	43.29	0.3	104.70	0.6	87.69	0.6	125.94	0.8	173.94	1.1
Barren land	12.78	0.1	11.02	0.1	2.70	0.1	1.55	0.0	3.03	0.0	3.02	0.0

3.2. Landscape Metrics Analysis

Landscape indices at a type level and the wetland area in the study area over 1975–2013 are illustrated in Table 3 (also see Table A5). All landscape indices in the study area fluctuated slightly during most investigated periods except for the period of 1975–2000, when there was a massive degradation in wetlands. Obviously, the values obtained for all indices showed that the artificial landscape experienced dramatic changes. The dominant landscapes existed in the early and later periods but changed significantly over the investigated years.

Table 3. Landscape metrics for the landscape pattern dynamics from 1975 to 2013 in the study area.

Year	LPI	SHAPE_MN	CONTIG_MN	FRAC_MN	PD	COHESION	SHDI	SHEI
1975	57.71	1.50	0.72	1.07	0.97	99.92	1.10	0.48
1983	32.28	1.43	0.70	1.06	1.34	99.90	1.25	0.54
1989	23.47	2.00	0.80	1.10	0.45	99.81	1.18	0.51
2000	45.77	2.09	0.78	1.11	0.47	99.90	1.03	0.45
2006	69.41	2.21	0.79	1.11	0.32	99.94	0.93	0.41
2013	62.95	1.75	0.62	1.10	1.41	99.92	1.01	0.44

Specifically, the largest patch index (LPI) tended to decrease between 1975 and 1989, and then to increase to 62.95 from 1989 to 2013, and it fluctuated with increase trends over 1989–2013. The mean patch shape index (SHAPE_MN) was larger than 1.43; SHAPE_MN increased from 1.50 to 2.21 from 1975 to 2006 and then decreased to 1.75. The change tendency of the average values of the contiguity index distribution (CONTIG_MN) and of the fractal dimension (FRAC_MN) of the research area fluctuated slightly, except for the period of 1983–1989, in which CONTIG_MN increased. The patch density (PD) increased from 0.97 in 1975 to 1.34 in 1983, then decreased to 0.32 in 2006, increasing at last to 1.41 in 2013. Similar to the changes in FRAC_MN, the patch cohesion index (COHESION) had no obvious changes and fluctuated slightly between 99.80 and 99.95, while the trend of COHESION declined in the early period but increased later. The landscape dominance index (SHDI) increased from 1.10 in 1975 to 1.25 in 1983, then declined to 0.93 in 2006 and stayed at 1.01 in 2013. Similar to the SHDI changes, the landscape evenness index (SHEI) increased from 0.48 in 1975 to the highest point of 0.54 in 1983 but declined to 0.41 in 2006 and stayed at 0.44 in 2013.

3.3. Regression of the Driving Forces of Wetlands Change Analysis

Pixels of wetland loss were significantly associated with distance to LULC in the six periods of 1975–1983, 1983–1989, 1989–2000, 2000–2006, 2006–2013, and 1975–2013. The relationship between pixels of wetland degradation and their distance to artificial lands (i.e., arable land, canal, transportation land, residential land) are illustrated in Figure 3.

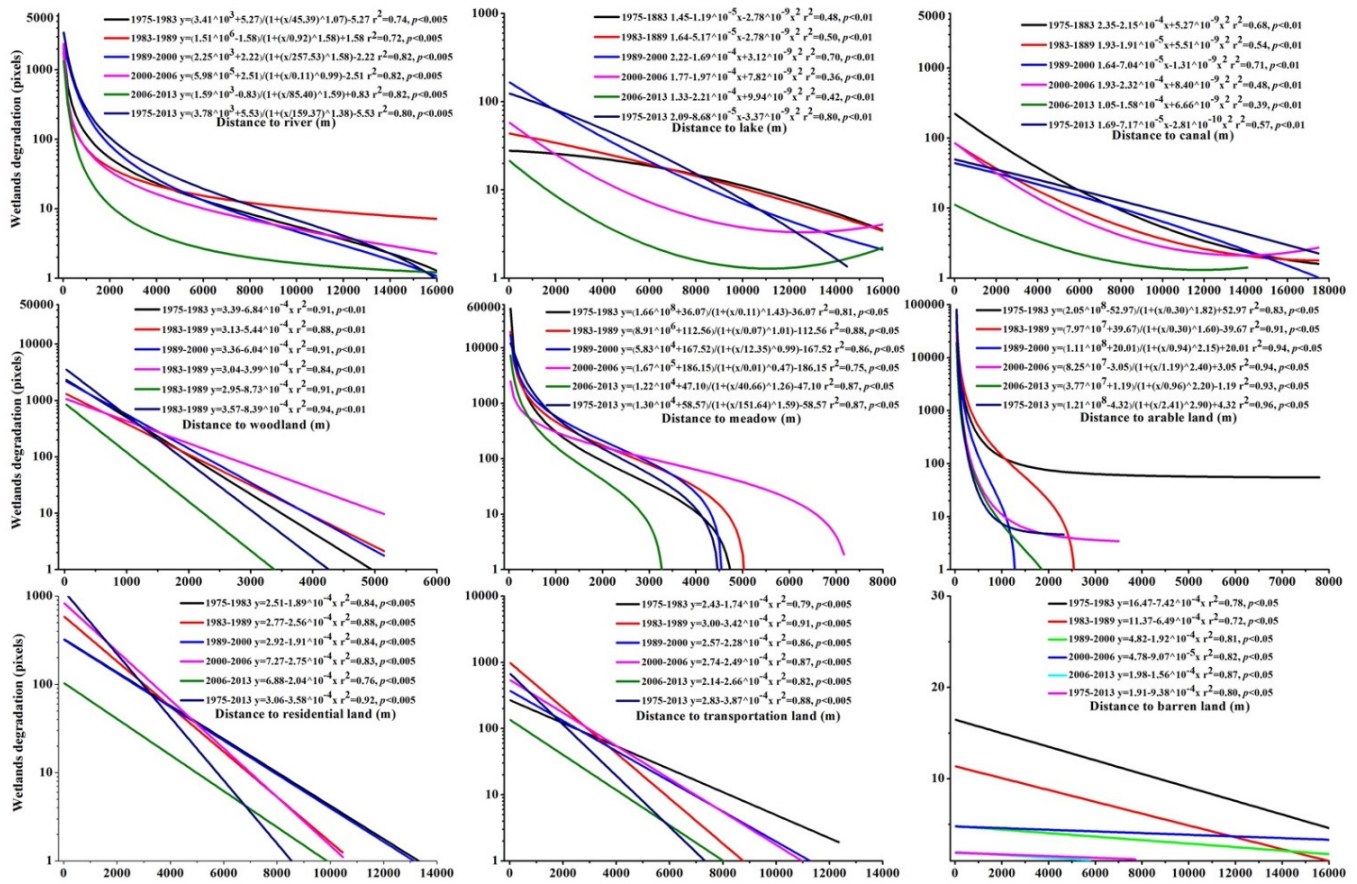


Figure 3. The trend between the loss of wetlands and the distance to other land covers (i.e., river, lake, canal, woodland, meadow, arable land, residential land, and barren land) in various periods from 1975–2013.

In the study area, the level of decrease in wetlands reduced sharply with the distance from arable land. The degradation rate of the wetland areas decreased in direct proportion to their distance, and the rate decreased rapidly at distances of less than 1.5 km from arable land. At more than 2.5 km, there were no obvious effects on wetland decrease from arable land. The distance from the pixels of the center patterns of the wetland to the nearest arable land always had a strong effect on wetland change from 1975 to 2013. The effect of arable land became weaker through all five periods in general, and the strongest effect on wetlands from arable land occurred during 1976–1983, while the weakest effect occurred during 2006–2013. During the six periods from 1975 to 2013, the longest distance effect period was 1975–1983, and the shortest distance effect period was 1989–2000.

From the regression analysis between the pixels of the lost wetland patterns and their distance to other artificial landscapes (i.e., canal, residential land, and transportation land), we found that distance to those lands had an unobvious relationship with the pixels of wetland reduction (Figure 3), and the pixels of wetlands decreased slowly with the increase in their distance to those landscapes. During the investigated 38 years and over the five periods, the decrease rate of the wetland area gradually reduced with distance, and the reduction rate rapidly decreased at distances larger than 6 km from canals. The regression trend in 2006–2013 had no significant decline changes. Compared with the distance of wetlands from canals, the pixels of wetlands lost to residential and transportation land also decreased slowly, but in a straight line. Figure 3 shows that the loss rate of the wetland area gradually reduced with its distance from residential and transportation land, which had limited effects on wetland loss when greater than 8 km. The effect of residential and transportation land became marginal with the shift of different periods (from 1975 to 2013), while the weakest period was 2006–2013.

The relationship between the pixels of lost wetlands and their distance from nature land cover had a significantly negative relationship with pixels of wetland decrease. Interestingly, the reduction rate of the pixels in wetland areas directly decreased with increasing distance and rapidly decreased at distances <1 km from the meadow, a more serious decline than other natural landscapes in the study area. When farther away than 5 km, the meadow had no significant effect on wetland decrease in the various periods. The distance to the nearest meadow always had a strong effect on the pixels of wetlands reduction from 1975 to 2013. The effects of the meadow became weak through all five periods. The strongest period was 1975–1983, while the weakest was 2006–2013. During the six periods from 1975 to 2013, the longest distance effect period was 2000–2006, while the weakest was 2006–2013. Second to the meadow, the effect of the nearest woodland on the pixels of wetlands reduction decreased slowly but straightforwardly from 1975 to 2013 and had no effect when greater than 5 km. In addition, the effect of the woodland generally lessened as the distance changed in the six different periods from 1975 to 2013; the strongest distance effect period was 1975–1983, the weakest was 2006–2013.

The relationship of the pixels of wetland loss to their distance from the river (see Figure 3) was very noticeable in the study region. The change rate of wetland areas sharply decreased with their distance from rivers, and the reduction rate gradually lessened at distances greater than 4 km from rivers. Similar to the meadow, the distance of the pixels of the wetlands from the nearest meadow also shortened largely during the six periods from 1975 to 2013. The largest distance effect period was 1973–1983, while the weakest was 2006–2013. Compared with rivers, the relationship between the pixels of wetland reduction and the distance from lake and barren land were insignificant and changed slightly in the study region.

4. Discussion

In the study areas, the land-use/land-cover (LULC) experienced significant conversions largely resulting from human activities during the period of 1975–2013 (see Figure 2 and Table A3). In brief, the areas of artificial land, including arable land, canals, residential and transportation land, increased; however, the areas of wetlands, meadow, and woodland were significantly degraded. The results of the previous analysis of the driving forces illustrated that there were several complicated causation factors in wetland degradation and that the spatiotemporal changes of wetland loss were the result of both natural controls and human-driven forces in the Sanjiang Plain [2,5,12,20,22]. However, our findings suggested that the main driving forces of wetland reduction are human activities, which should be primarily analyzed rather than considering many additional factors. The noticeable decrease in wetlands and the associated increase in arable land were considered to have a close relationship with the rapidly increasing commercial agricultural product [16,40]; arable land reclamation for grain production was the main threat to the wetlands in the Sanjiang Plain over the past decades [5]. The most noticeable LULC change was the rapid decrease in wetlands versus the rapid increase in arable land. Over the investigated period, wetland losses of 8012.32 km² were accompanied by the substantial expansion of arable lands (Figure 2). Wetlands located in areas with various elevations and different distances from artificial land and open water [21,35] have been converted to arable land starting with the easy reclamation areas and moving to difficult areas, from high elevations to low, and from river terraces to floodplains as well as meander belts [15]. Considerable wetland loss and fragmentation occurred in the period of 1975–1983 (Tables Tables A2 and A3). However, the rates of wetland loss and arable land increase slowed down after 2000. The landscape metrics index changed dramatically from 1975 to 2013, probably because the causes of wetland fragmentation differed in various periods. Wetlands were the largest landscape patch in 1975, then decreased and were converted to other landscapes but mainly to arable land; at last, the arable land became the dominant landscape in 2013. We agree with Zhang et al. (2009) that wetland degradation can be categorized as, on the one hand, direct loss attributed to LULC conversion and, on the other hand, indirect loss owing to

the wetlands quality decline, especially diversion of the water supply from irrigation of arable lands and drainage of canals [12]. A high correlation between natural land decrease and artificial land increase in anthropogenic activities was observed from 1975 to 2013; the landscape changed considerably, especially the increased arable land versus the wetland reclamation, and water continued to be drained for arable land development in the study area (see Figures 2 and 3).

More specifically, in 1975 wetlands covered 10,126.18 km², or 63.0%, of the total study area. In the 1980s, the Sanjiang Plain entered into a long period of agricultural modernization, popularized an advanced agricultural machinery pilot project, and built up large, modernized farms [41]. This period was the cultivation and agriculture development peak lasting until the beginning of the 1980s and involved the degradation of 2471.14 km² of wetlands, and 2315.66 km² arable land was converted from wetlands from 1975 to 1983. In the period between the mid-1980s and 2000, the market-oriented economy became the dominant system because the Sanjiang Plain was one of the most important agricultural production bases, not only for itself but also for supporting a huge amount of trade with other provinces [3]. Meanwhile, the reductions in plant species richness and biology amplified the threats of reductions in plants, animals, and, in particular, rare birds that have been led by wetland degradation [42]. For instance, foraging and reproduction of waterfowl could be affected by the fragmentation and loss of wetlands, as well as their patch change and isolation [5,12].

Fortunately, with the universally increasing consciousness of the functions and purposes of wetland ecosystems and the ecological consequences of wetland degradation in the 1990s, Chinese governments attempted to prohibit wetlands reclamation and to establish nature reserves in the Sanjiang Plain [20]. From 1985 to 2003, several national and provincial reserves for wetlands were established in the study area [3,20]; the HNNR was approved in 2000, and the SNNR was approved in 2000, both of them were listed as Ramsar wetlands in 2002. While the degradation of wetlands was not stopped until 2006, consequently, the conversion speed of wetlands has been reduced ever since [3,19]. Since 2005, the Degraded Wetland Restoration Program (DWRP) and the National Wetland Conservation Program (NWCP) have been implementing by the Chinese Government in order to protect natural wetlands from reclamation and to transform low-yield arable lands into natural wetlands [20]. In addition, increased abandonment of arable land owing to the migration of farming laborers to the urban regions was reverted after the implementation of this policy [19].

Economic growth depends mainly on grain production, and most local people in the study area make a living by farming. The expansion of arable land converted from wetlands can improve the economic situations of local shareholders. On average, population density was approximately 13 person/km² in 1976, but it grew to 79 person/km² in 2005 in the Sanjiang Plain [19]. Figure 2 shows that the area of settlement and transportation systems increased rapidly during the period of 1975–2013 in the study area. The previous analysis indicated that wetlands were largely lost to arable land (see Table A4 for detail). This process most likely led to a worse effect on wetlands because the increase in population would cause the conversion of wetlands into arable land. The growing agricultural economy will subsequently encourage local agricultural people to continue to reclaim wetlands. With large-scale agricultural development, wetlands have been converted directly into agricultural land by tilling and planting, and most wetlands in the study areas have been either fragmented or isolated [15]. We can also conclude from the results of the regression of driving forces analysis that wetland reduction near artificial land has been more serious than that further from artificial lands (Table 2). However, compared with the effect of artificial land, the natural land's effect on wetland reduction has been less severe, and the weakest effect on wetlands from natural land came from the lake and barren land. The level of reduction in the wetland areas had no obvious change with long distance to both lake and barren land. This means that wetland reduction near the lake and barren land had no relationship to the distance from the lake and barren land.

Compared with direct loss resulting from LULC conversion, indirect effects usually resulted in water loss from wetlands, which were degraded as wet meadow or meadow [13,14,27,34]. The indirect loss mainly resulted from the decline in the environmental quality of wetlands, especially the diversion of the water supply for canals and irrigation [12]. Farming is the largest consumer of water resources in the world, and approximately 85.0% of all water is consumed by human beings [2]. Therefore, hydraulic projects resulted from the agriculture growth. Canal systems can interrupt the natural hydrologic distribution of the basins and undermine their integrity, leading to structural dynamics in the basins landscapes in wetlands [22]. Many agricultural canals were constructed to dry wetlands and irrigate arable land in the study area (see Figure 2). From 1975 to 2013, the canal system was directly increasing, which was one cause of the dynamic changes in wetland landscapes (Table A3). Paddy fields expanded considerably for local farmers during the study period, while there were few paddy fields before 1979 in the Sanjiang Plain [2]. As paddy fields that produce rice are more profitable than dry arable land, a number of dry lands were converted to paddy fields. Rather than continue to reclaim cultivable land from wetlands and reinforce wetland protection regulations, suitable wetland covers remaining for cultivation were minified beside the wetlands in the natural reserves.

5. Conclusions and Implications

In this paper, based on remotely sensed data sets using GIS approaches and statistical methods, the spatial and temporal trajectories of wetland reduction and LULC change were analyzed in the Sanjiang Plain north of the Wandashan Mountains, China. Wetlands occupied 63.0% of the study area as the dominant landscape in 1975 but fell to 13.8% in 2013 as lost wetlands were converted to other land covers, especially arable land coverage. Our results suggested that the drastic changes in wetlands were attributed to the socio-economic conditions and human activities, and the largest driving force was agricultural cultivation over severe effects of agricultural reclamation, which played a crucial role in the reduction in and degradation of wetlands. Based on our landscape change investigation, the closer to arable land, the worse the wetland loss over the entire study period. Fortunately, after 2000, with the governmental policies aimed at protecting and restoring implementation for wetlands, the rate of wetland loss declined slightly over the later time intervals (between 2000 and 2013) in the study area.

This finding may inspire researchers to understand the driving forces of wetland reduction in other regions, which will be helpful for the management and protection of wetlands. As some natural habitats with a large number of fauna are located in natural wetland parks, and landscapes are dominated by arable land intended for feeding a huge number of people in or out of the Sanjiang Plain, future actions by both governments and individuals will be required to balance agricultural production and wetland protection for further sustainable development.

Author Contributions: All authors contributed to the development of the research and the elaboration of this article. Specifically, conceptualization, J.X.; methodology, J.X., Y.S. and X.L.; software, J.X. and Y.S.; validation, J.X. and Y.S.; investigation, J.X., Z.D., M.L. and X.L.; data curation, Z.D., Y.S. and X.L.; writing—original draft preparation, J.X., Z.D., M.L. and X.L.; writing—review and editing, J.X., Y.S. and X.L.; supervision, Y.S. and X.L.; funding acquisition, X.L. All authors have read and agreed to the published version of the manuscript.

Funding: This research is funded by the National Natural Science Foundation of China (Grant No. 52108011); China Postdoctoral Science Foundation (Grant No. 2021M701249); Department of Education of Guangdong Province (Grant No. 2021KTSCX004); Science and Technology Program of Guangzhou, China (Grant No. 202102020302); Department of Housing and Urban–Rural Development of Guangdong Province (Grant No. 2021-K2-305243); State Key Laboratory of Subtropical Building Science, South China University of Technology (Grant No. 2021ZB16 and Grant No. 2022ZA01); Transverse Scientific Research Projects of South China University of Technology (Grant No. x2jzD8197240 and Grant No. x2jzD8205910).

Institutional Review Board Statement: Not applicable.

Informed Consent Statement: Not applicable.

Data Availability Statement: The data supporting the findings of this research are available within the article.

Acknowledgments: The authors thank the editors and the anonymous reviewers for their helpful recommendations for improving this article.

Conflicts of Interest: The authors declare no conflict of interest.

Appendix A

Table A1. Landsat images covering the study area.

Year	Sensor	Date (Day/Month)	Band No.	Path/Row	Year	Sensor	Date	Band No.	Path/Row
1975	Landsat MSS	31/05	1,2,3,4	122/26	2000	Landsat-7 ETM+	15/09	1, 2, 3, 4, 5, 8	113/26
	Landsat MSS	24/07	1,2,3,4	122/27		Landsat-7 ETM+	11/06	1, 2, 3, 4, 5, 8	113/27
	Landsat MSS	25/07	1,2,3,4	123/27		Landsat-7 ETM+	04/07	1, 2, 3, 4, 5, 8	114/27
1983	Landsat MSS	16/08	1,2,3,4	113/26	2006	Landsat-5 TM	24/09	1, 2, 3, 4, 5	113/26
	Landsat MSS	16/08	1,2,3,4	113/27		Landsat-5 TM	24/09	1, 2, 3, 4, 5	113/27
	Landsat MSS	23/08	1,2,3,4	114/27		Landsat-5 TM	30/08	1, 2, 3, 4, 5	114/27
1989	Landsat-5 TM	09/09	1, 2, 3, 4, 5	113/26	2013	Landsat-8	23/06	2, 3, 4, 5, 6, 8	113/26
	Landsat-5 TM	09/09	1, 2, 3, 4, 5	113/27		Landsat-8	27/09	2, 3, 4, 5, 6, 8	113/27
	Landsat-5 TM	16/09	1, 2, 3, 4, 5	114/27		Landsat-8	18/09	2, 3, 4, 5, 6, 8	114/27

Table A2. Accuracy of classification.

Year	Overall Accuracy	Kappa
1975	76.2%	0.712
1983	75.1%	0.702
1989	78.3%	0.721
2000	82.4%	0.735
2006	83.2%	0.737
2013	85.5%	0.753

Table A3. Changes in land-use/land-cover (LULC) area (%) and annual change (km²/year) during different periods of 1975–2013.

LULC Types	Changes in LULC Area (%)					Annual Change (km ² /Year)						
	1975–1983	1983–1989	1989–2000	2000–2006	2006–2013	1975–2013	1975–1983	1983–1989	1989–2000	2000–2006	2006–2013	1975–2013
Wetland	−24.4	−25.4	−44.2	−28.6	−2.6	−78.1	−308.89	−323.71	−229.69	−151.90	−8.57	−208.19
River	−8.5	9.3	−14.7	4.2	3.0	−8.4	−4.15	5.53	−5.23	2.33	1.50	−0.87
Lake	−36.4	4.8	62.2	−4.0	−8.6	−5.3	−1.42	0.16	1.17	−0.23	−0.40	−0.04
Canal	260.8	43.6	49.6	30.7	30.6	1222.0	1.45	1.16	1.04	1.76	1.97	1.43
Woodland	−1.0	4.5	−3.8	2.3	9.5	11.5	−1.57	9.28	−4.41	4.79	17.20	3.79
Meadow	786.7	−94.6	−29.3	−64.6	172.4	−67.4	848.96	−1207.17	−10.96	−31.35	25.44	−15.31
Arable land	63.9	47.3	33.9	9.2	−2.7	243.3	265.15	428.88	247.08	164.58	−45.73	212.62
Residential land	54.1	105.6	33.0	17.1	14.6	465.2	1.88	7.56	2.65	3.35	2.86	3.41
Transportation land	15.8	141.9	−16.2	43.6	38.1	365.5	0.74	10.24	−1.55	6.37	6.86	3.59
Barren land	−13.8	−75.5	−42.6	95.5	−0.3	−76.4	−0.22	−1.39	−0.10	0.25	−0.00	−0.26

Table A4. Areas (km²) and percentages of wetlands converted into non-wetland landscapes during the six time intervals.

LULC Conversion	1975–1983		1983–1989		1089–2000		2000–2006		2006–2013		1975–2013	
	Area	%	Area	%	Area	%	Area	%	Area	%	Area	%
River	10.37	0.3	11.57	0.4	1.30	0.1	4.10	0.4	7.20	2.7	11.15	0.1
Lake	0.79	0.0	2.87	0.1	8.45	0.3	1.13	0.1	0.84	0.3	3.78	0.1
Canal	4.52	0.1	1.06	0.0	0.88	0.0	1.38	0.1	0.37	0.1	10.05	0.1
Woodland	97.40	3.1	225.14	7.8	120.87	4.3	39.73	4.2	21.17	8.1	161.43	2.0
Meadow	719.42	22.8	225.71	7.8	89.18	3.1	12.83	1.4	5.22	2.0	20.77	0.3
Arable land	2315.66	73.4	2427.72	83.7	2620.49	92.1	896.75	93.7	226.33	86.2	8012.32	97.3
Residential land	3.81	0.1	1.78	0.1	2.18	0.1	0.22	0.0	0.55	0.2	14.79	0.2
Transportation land	3.27	0.1	3.42	0.0	1.33	0.1	0.45	0.1	0.79	0.3	4.14	0.1
Barren land	0.83	0.0	0.04	0.0	0.14	0.0	0.06	0.0	0.00	0.0	0.00	0.0

Table A5. The characteristics of 10 landscape types in 2013.

Landscape Category	LULC Types	Perimeter of Each LULC Type (km)	Number of Patches
Natural landscapes	Wetland	10,809.90	1822
	Woodland	1393.27	7270
	Meadow	281.43	1043
	River	2735.63	144
	Lake	289.85	77
	Barren land	11.16	2
	Arable land	31,545.12	2509
Artificial landscapes	Residential land	1770.23	616
	Transportation land	7052.20	1508
	Canal	1607.17	69
Total		82,223.90	15,060

References

- Mitra, S.; Wassmann, R.; Vlek, P.L.G. An appraisal of global wetland area and its organic carbon stock. *Curr. Sci.* **2005**, *88*, 25–35.
- Song, K.; Wang, Z.; Du, J.; Liu, L.; Zeng, L.; Ren, C. Wetland Degradation: Its Driving Forces and Environmental Impacts in the Sanjiang Plain, China. *Environ. Manag.* **2014**, *54*, 255–271. [\[CrossRef\]](#)
- Wang, Z.; Zhang, B.; Zhang, S.; Li, X.; Liu, D.; Song, K.; Li, J.; Li, F.; Duan, H. Changes of Land Use and of Ecosystem Service Values in Sanjiang Plain, Northeast China. *Environ. Monit. Assess.* **2006**, *112*, 69–91. [\[CrossRef\]](#) [\[PubMed\]](#)
- Jeng, H.; Hong, Y.-J. Assessment of A Natural Wetland for Use in Wastewater Remediation. *Environ. Monit. Assess.* **2005**, *111*, 113–131. [\[CrossRef\]](#) [\[PubMed\]](#)
- Wang, Z.; Song, K.; Ma, W.; Ren, C.; Zhang, B.; Liu, D.; Chen, J.M.; Song, C. Loss and Fragmentation of Marshes in the Sanjiang Plain, Northeast China, 1954–2005. *Wetlands* **2011**, *31*, 945–954. [\[CrossRef\]](#)
- Foley, J.A.; DeFries, R.; Asner, G.P.; Barford, C.; Bonan, G.; Carpenter, S.R.; Chapin, F.S.; Coe, M.T.; Daily, G.C.; Gibbs, H.K.; et al. Global consequences of land use. *Science* **2005**, *309*, 570–574. [\[CrossRef\]](#)
- Fu, J.; Liu, J.; Wang, X.; Zhang, M.; Chen, W.; Chen, B. Ecological risk assessment of wetland vegetation under projected climate scenarios in the Sanjiang Plain, China. *J. Environ. Manag.* **2020**, *273*, 111108. [\[CrossRef\]](#) [\[PubMed\]](#)
- Seidl, A.F.; Moraes, A.S. Global valuation of ecosystem services: Application to the Pantanal da Nhecolandia, Brazil. *Ecol. Econ.* **2000**, *33*, 1–6. [\[CrossRef\]](#)
- Sui, X.; Zhang, R.; Frey, B.; Yang, L.; Li, M.-H.; Ni, H. Land use change effects on diversity of soil bacterial, Acidobacterial and fungal communities in wetlands of the Sanjiang Plain, northeastern China. *Sci. Rep.* **2019**, *9*, 18535. [\[CrossRef\]](#) [\[PubMed\]](#)
- He, B.-J.; Wang, J.; Liu, H.; Ulpiani, G. Localized synergies between heat waves and urban heat islands: Implications on human thermal comfort and urban heat management. *Environ. Res.* **2020**, *193*, 110584. [\[CrossRef\]](#)
- He, B.-J. Potentials of meteorological characteristics and synoptic conditions to mitigate urban heat island effects. *Urban Clim.* **2018**, *24*, 26–33. [\[CrossRef\]](#)
- Zhang, S.; Na, X.; Kong, B.; Wang, Z.; Jiang, H.; Yu, H.; Zhao, Z.; Li, X.; Liu, C.; Dale, P. Identifying wetland change in China's Sanjiang Plain using remote sensing. *Wetlands* **2009**, *29*, 302–313. [\[CrossRef\]](#)
- Mao, D.; Wang, Z.; Du, B.; Li, L.; Tian, Y.; Jia, M.; Zeng, Y.; Song, K.; Jiang, M.; Wang, Y. National wetland mapping in China: A new product resulting from object-based and hierarchical classification of Landsat 8 OLI images. *ISPRS J. Photogramm. Remote Sens.* **2020**, *164*, 11–25. [\[CrossRef\]](#)
- Mao, D.; Tian, Y.; Wang, Z.; Jia, M.; Du, J.; Song, C. Wetland changes in the Amur River Basin: Differing trends and proximate causes on the Chinese and Russian sides. *J. Environ. Manag.* **2020**, *280*, 111670. [\[CrossRef\]](#)

15. Liu, J.; Sheng, L.; Lu, X.; Liu, Y. A dynamic change map of marshes in the Small Sanjiang Plain, Heilongjiang, China, from 1955 to 2005. *Wetl. Ecol. Manag.* **2014**, *23*, 419–437. [[CrossRef](#)]
16. Yan, F.; Zhang, S. Ecosystem service decline in response to wetland loss in the Sanjiang Plain, Northeast China. *Ecol. Eng.* **2019**, *130*, 117–121. [[CrossRef](#)]
17. Ramsar Convention Secretariat. *The Ramsar Convention Manual*, 6th ed.; Ramsar Convention Secretariat: Gland, Switzerland, 2013.
18. Gong, P.; Niu, Z.; Cheng, X.; Zhao, K.; Zhou, D.; Guo, J.; Liang, L.; Wang, X.; Li, D.; Huang, H.; et al. China's wetland change (1990–2000) determined by remote sensing. *Sci. China Earth Sci.* **2010**, *53*, 1036–1042. [[CrossRef](#)]
19. Song, K.; Liu, D.; Wang, Z.; Zhang, B.; Jin, C.; Li, F.; Liu, H. Land use change in Sanjiang Plain and its driving forces analysis since 1954. *Dili Xuebao/Acta Geogr. Sin.* **2008**, *63*, 93.
20. Xiang, H.; Wang, Z.; Mao, D.; Zhang, J.; Xi, Y.; Du, B.; Zhang, B. What did China's National Wetland Conservation Program Achieve? Observations of changes in land cover and ecosystem services in the Sanjiang Plain. *J. Environ. Manag.* **2020**, *267*, 110623. [[CrossRef](#)]
21. Xie, J.; Wang, Z.M.; Mao, D.H.; Ren, C.Y.; Han, J.X. Remote sensing classification of Wetlands using Object-oriented method and Multi-season HJ-1 Images—A case study in the Sanjiang plain North of the Wandashan Mountain. *Wetl. Sci.* **2012**, *10*, 429–438.
22. Wang, G.; Jiang, M.; Wang, M.; Xue, Z. Natural revegetation during restoration of wetlands in the Sanjiang Plain, Northeastern China. *Ecol. Eng.* **2019**, *132*, 49–55. [[CrossRef](#)]
23. Brown, M.T.; Vivas, M.B. LANDSCAPE DEVELOPMENT INTENSITY INDEX. *Environ. Monit. Assess.* **2005**, *101*, 289–309. [[CrossRef](#)]
24. Li, B.; Guo, W.; Liu, X.; Zhang, Y.; Russell, P.J.; Schnabel, M.A. Sustainable Passive Design for Building Performance of Healthy Built Environment in the Lingnan Area. *Sustainability* **2021**, *13*, 9115. [[CrossRef](#)]
25. Findlay, C.S.T.; Bourdages, J. Response Time of Wetland Biodiversity to Road Construction on Adjacent Lands. *Conserv. Biol.* **2000**, *14*, 86–94. [[CrossRef](#)]
26. Forman, R.T.T.; Deblinger, R.D. The Ecological Road-Effect Zone of a Massachusetts (U.S.A.) Suburban Highway. *Conserv. Biol.* **2000**, *14*, 36–46. [[CrossRef](#)]
27. Jia, M.; Mao, D.; Wang, Z.; Ren, C.; Zhu, Q.; Li, X.; Zhang, Y. Tracking long-term floodplain wetland changes: A case study in the China side of the Amur River Basin. *Int. J. Appl. Earth Obs. Geoinf.* **2020**, *92*, 102185. [[CrossRef](#)]
28. Rebelo, L.-M.; Finlayson, C.; Nagabhatla, N. Remote sensing and GIS for wetland inventory, mapping and change analysis. *J. Environ. Manag.* **2009**, *90*, 2144–2153. [[CrossRef](#)] [[PubMed](#)]
29. Ordoyone, C.; Friedl, M.A. Using MODIS data to characterize seasonal inundation patterns in the Florida Everglades. *Remote Sens. Environ.* **2008**, *112*, 4107–4119. [[CrossRef](#)]
30. He, B.-J.; Zhao, Z.-Q.; Shen, L.-D.; Wang, H.-B.; Li, L.-G. An approach to examining performances of cool/hot sources in mitigating/enhancing land surface temperature under different temperature backgrounds based on landsat 8 image. *Sustain. Cities Soc.* **2018**, *44*, 416–427. [[CrossRef](#)]
31. Tang, X.; Ding, Z.; Li, H.; Li, X.; Luo, J.; Xie, J.; Chen, D. Characterizing ecosystem water-use efficiency of croplands with eddy covariance measurements and MODIS products. *Ecol. Eng.* **2015**, *85*, 212–217. [[CrossRef](#)]
32. Zhao, D.; Zhao, X.; Khongnawang, T.; Arshad, M.; Triantafilis, J. A Vis-NIR Spectral Library to Predict Clay in Australian Cotton Growing Soil. *Soil Sci. Soc. Am. J.* **2018**, *82*, 1347–1357. [[CrossRef](#)]
33. Zhao, D.; Arshad, M.; Wang, J.; Triantafilis, J. Soil exchangeable cations estimation using Vis-NIR spectroscopy in different depths: Effects of multiple calibration models and spiking. *Comput. Electron. Agric.* **2021**, *182*, 105990. [[CrossRef](#)]
34. Jia, M.; Wang, Z.; Mao, D.; Ren, C.; Wang, C.; Wang, Y. Rapid, robust, and automated mapping of tidal flats in China using time series Sentinel-2 images and Google Earth Engine. *Remote Sens. Environ.* **2021**, *255*, 112285. [[CrossRef](#)]
35. Xie, J.; Wang, Z.M.; Ren, C.Y. Analysis of seasonal changes of wetland landscape patterns derived from remote sensing data. *Shengtai Xuebao/Acta Ecol. Sin.* **2014**. [[CrossRef](#)]
36. Baatz, M.; Schape, A. Multiresolution Segmentation—An Optimization Approach for High Quality Multi-Scale Image Segmentation Angewandte Geographische Informationsverarbeitung XII. Available online: <https://www.semanticscholar.org/paper/Multiresolution-Segmentation-%3A-an-optimization-for-Baatz-Sch%C3%A4pe/364cc1ff514a2e11d21a101dc072575e5487d17e> (accessed on 22 November 2021).
37. Benz, U.C.; Hofmann, P.; Willhauck, G.; Lingenfelder, I.; Heynen, M. Multi-resolution, object-oriented fuzzy analysis of remote sensing data for GIS-ready information. *ISPRS J. Photogramm. Remote. Sens.* **2004**, *58*, 239–258. [[CrossRef](#)]
38. McGarigal, K.; Marks, B.J. FRAGSTATS: Spatial Pattern Analysis Program for Quantifying Landscape Structure. Available online: <https://www.fs.usda.gov/treesearch/pubs/3064> (accessed on 22 November 2021).
39. Ramezani, H.; Holm, S. Sample based estimation of landscape metrics; accuracy of line intersect sampling for estimating edge density and Shannon's diversity index. *Environ. Ecol. Stat.* **2009**, *18*, 109–130. [[CrossRef](#)]
40. Mao, D.; Wang, Z.; Wu, J.; Wu, B.; Zeng, Y.; Song, K.; Yi, K.; Luo, L. China's wetlands loss to urban expansion. *Land Degrad. Dev.* **2018**, *29*, 2644–2657. [[CrossRef](#)]
41. Li, Y.; Wei, Y.D. The spatial-temporal hierarchy of regional inequality of China. *Appl. Geogr.* **2010**, *30*, 303–316. [[CrossRef](#)]
42. Liu, H.; Zhang, S.; Li, Z.; Lu, X.; Yang, Q. Impacts on Wetlands of Large-scale Land-use Changes by Agricultural Development: The Small Sanjiang Plain, China. *AMBIO* **2004**, *33*, 306–310. [[CrossRef](#)]